

Investigation of Fusion Hindrance in the decay of Pre-actinide $^{204}\text{Po}_{84}$ Nuclear system

Thesis submitted in partial fulfillment of the requirement for

The award of the degree of

Masters of Science

In

PHYSICS

Under

The supervision of

Dr. Manoj K Sharma

Submitted by

Nandni Sharma

Roll no: 300804021



School of physics and Material Science

Thapar University

Patiala-147001 (Punjab)

July 2010

DEDICATION

This dissertation work is dedicated to my wonderful parents, Mr. Ramesh Kumar Bhardwaj and Mrs. Shobha Sharma, who have raised me to be the person I am today. They taught me that the best kind of knowledge to have, is that which is learnt for its own sake and that the largest task can be accomplished if it is done one step at a time.

I also thank my beloved grandparents, Mr. Som Datt and Mrs. Gayatri Devi, and my brother Nishant Sharma for their never ending moral support and prayers which always acted as catalyst in my academic life.

Finally this work is dedicated to all those who believe in richness of learning.

CERTIFICATE

This is to certify that Ms. Nandni Sharma, Roll No.300804021 has worked on this thesis report as a partial fulfillment for award of the degree of MASTERS OF SCIENCE in physics. I certify that the matter embodied in this report is of candidate's own record and not submitted to any other university in any part or full form for the award of such a degree.



Dr. Manoj K Sharma

Supervisor

SPMS, Thapar University

Patiala

Countersigned by:



Dr. O.P. Pandey

(Prof. & Head)

School of Physics and Material Science

Thapar University, Patiala



Dr. R.K. Sharma

Dean of academic affairs

Thapar University

Patiala

Acknowledgement

I owe my deepest gratitude to **Dr. Manoj Sharma**, *my worthy supervisor*, without him the dissertation would not have been possible. I thank him for his patience and encouragement that carried me on through difficult times, and for his insights and suggestions that helped to shape my research skills. I express my sincere thanks to him for his valuable guidance in carrying out under his effective supervision, encouragement and cooperation. His visionary thoughts have influenced me greatly. His dynamical attitude has empowered me with zeal of energy to conquer the finer details of my research work.

I also thank **Dr. O.P Pandey, Professor & Head**, school of physics and material science for his support and providing facilities.

A special word of thanks to **Ms. Gudveen**, research scholar for the help and valuable suggestions whenever I need it out for her busy schedule.

Special thanks to all my friends and the staff at the school of physics and material sciences for providing me a friendly atmosphere and encouraging me throughout this work. I am deeply thankful to my family, their moral support and patient has bore fruit through completion of this thesis.

Nandni Sharma

Roll No: 300804021

Abstract

In view of present day developments in the domain of theoretical nuclear physics, it is extremely important & essential to study the nuclear dynamics and related aspects at the extreme conditions of temperature, angular momentum, & energies in reference to recent advances in the field of experimental nuclear physics. One of the important aspects in this category is the fusion hindrance. Fusion hindrance in pre-actinide region is currently an active area of investigation as majority of nuclei in this mass region respond to this kind of mechanism. We have investigated the fusion hindrance in the decay of ^{204}Po formed in $^{16}\text{O}+^{188}\text{Os}$ reaction using the Dynamical Cluster decay Model (DCM). We have calculated the evaporation residue and Fission cross section in reference to available experimental data. As expected investigated nuclear reaction does not lead to fusion hindrance at the selected range of incident energies.

CONTENTS

Certificate	3
Acknowledgement	4
Abstract	5
CHAPTER-1 INTRODUCTION	9
1.1 Discovery of nuclear fission	10
1.2 Experiments to confirm the idea of nuclear fission	11
1.3 Nuclear fission	11
1.4 Fission explained with the help of liquid drop model	13
1.5 Energy released in nuclear fission	15
1.6 Compound nucleus formation and its decay	17
1.6.1 Compound nucleus mechanism	17
1.7 Non compound nucleus	18
1.8 Fusion hindrance in heavy elements	20
1.9 Stability of nucleus	21
2.0 References	25
CHAPTER -2 METHODOLOGY	
2.1 Introduction of DCM	28
2.2 DCM for hot and rotating compound nucleus	29

2.2.1 Postulates of first turning point	31
2.2.2 The second turning point	32
2.3 Overview of potentials	34
2.3.1 The proximity potential	34
2.3.2 The coulomb potential	34
2.3.3 The angular momentum potential	35
2.4 Classical Hydrodynamical Mass Parameter	36
2.5 Preformation Probability P_0	38
2.6 Penetration Probability P	39
2.7 Assault Frequency ν_0	39
2.8 References	40
CHAPTER -3 Results and Discussions	
3.1 Introduction	44
3.2 Results and discussions	45
3.3 References	52

List of Figures

Fig.1.1 Isotopes of Hydrogen, Helium, Lithium and Sodium

Fig.1.2 Nuclear Fission Process

Fig.1.3 Potential barrier and Compound nucleus formation

Fig.1.1 Competing decay processes

Fig. 1.5 Decomposition of a nucleus into two fragments

Fig. 1.6 Potential barrier as a function of relative separation between fragments

Fig.2.1. Scattering Plot for $^{16}\text{O} + ^{188}\text{Os} \rightarrow ^{204}\text{Po}$ reaction

Fig.2.2. The geometry of classical hydrodynamical model for calculating mass parameter $B_{\eta\eta}$

Fig. 3.1 Fragmentation potential as a function of fragment mass

Fig. 3.2 Variation of Preformation probability as the function of mass fragments (A_2)

Fig. 3.3 Penetrability as the function of fragment mass number at $\ell=0\hbar$ and $\ell=132\hbar$

Fig. 3.4 Scattering Potential as a function of nuclear range

Fig. 3.5 Neck length parameter as a function of E_{CM}

Fig. 3.6 Cross sections as a function of E_{CM}

CHAPTER 1

INTRODUCTION

INTRODUCTION

Ernest Rutherford discovered that protons (positively charged particles) situated in the nucleus of the atom along with negatively charged electrons orbiting around the nucleus that makes the atom. After discovering the protons, there was one problem that the physicists couldn't explain why several elements weighed different amounts. In 1932, James Chadwick, discovered the neutron, a third subatomic particle [1]. Neutrons have no charge and they share space with protons in the nucleus of the atom. While the number of protons and electrons is always the same for any given element. For example carbon, there are always 14 protons and 14 electrons but there can be different numbers of neutrons. This explained why carbon could weigh different amounts, even though it was essentially the same element. These different weights of atoms are known as isotopes.

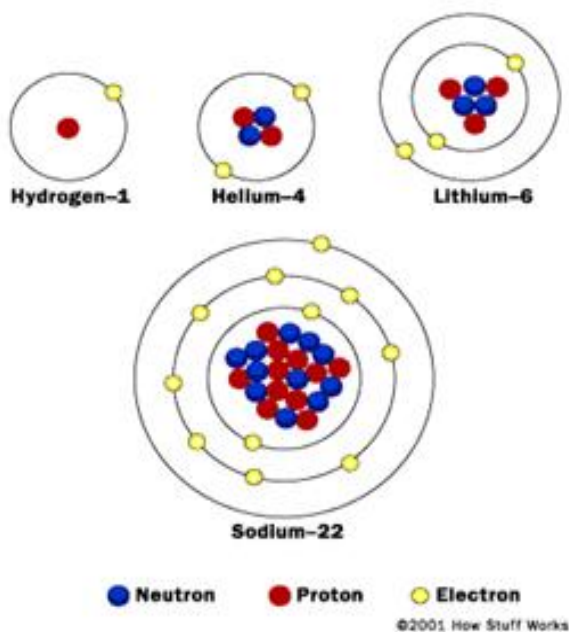


Figure 2.1 Isotopes of Hydrogen, Helium, Lithium and Sodium

1.1 Discovery of Nuclear Fission

Initially, the Scientists began using particle accelerators to bombard the nuclei of atoms in the hopes of splitting atoms and creating energy. They achieved very little success because the early particle accelerators shot out protons and alpha particles and they both are positively charged. Even at high speeds, these particles were easily repelled by the positively charged nuclei, and the likes of Rutherford, Albert Einstein and Niels Bohr felt that harnessing atomic power was close to impossible.

This changed when Italian physicist Enrico Fermi thought to use neutrons for bombardment in 1934. Since neutrons have no charge, they can hit an atom's nucleus without being repelled. Shortly thereafter, Enrico Fermi and his associates in Italy undertook an extensive investigation of the nuclear reactions produced by the bombardment of various elements with this uncharged particle [2]. In particular, they observed (1934) that at least four different radioactive species resulted from the bombardment of uranium with slow neutrons. These newly discovered species emitted beta particles and were thought to be isotopes of unstable "transuranium elements" of atomic numbers 93, 94, and perhaps higher [3]. There was of course, intense interest in examining the properties of these elements. Hahn and Strassmann published a scientific paper showing that small amounts of barium (element 56) were produced when uranium (element 92) was bombarded with neutrons. It was very puzzling to them how a single neutron could transform element 92 into element 56?

Lise Meitner suggested a helpful model for such a reaction. One can visualize the uranium nucleus to be like a liquid drop containing protons and neutrons. When an extra neutron enters, the drop begins to vibrate [4]. If the vibration is violent enough, the drop can break into two pieces. Meitner named this process "fission" because it is similar to the process of cell division in biology. It takes only a small amount of energy to start the vibration which leads to a major breakup.

1.2 Experiments to confirm the idea of nuclear fission

The two experiments were done by the Scientists to confirm the idea of nuclear fission.

(1) In one experiment, a thin sheet of uranium was placed inside a cloud chamber.

A cloud chamber is a device in which vapour trails of moving nuclear particles can be seen and photographed. When it was irradiated by neutrons, photographs showed a pair of tracks going in opposite directions from a common point in the uranium. Clearly, a nucleus had been photographed in the act of fission.

(2) In other experiment they used a Geiger counter, which is a small, cylindrical tube that produces electrical pulses when a radioactive particle passes through it. For this experiment, the inside of a modified Geiger tube was lined with a thin layer of uranium. When a neutron source was brought near it, large voltage pulses were observed, much larger than from ordinary radioactivity. When the neutron source was taken away, the large pulses stopped. A Geiger tube without the uranium lining did not generate large pulses. Evidently, the large pulses were due to uranium fission fragments. The size of the pulses showed that the fragments had a very large amount of energy.

In early experiments the uranium is bombarded with slow neutrons and it was rapidly established that the rare isotope uranium-235 was responsible for this phenomenon. The more abundant isotope uranium-238 could be made to undergo fission only by fast neutrons with energy exceeding 1 MeV. The nuclei of other heavy elements, such as thorium and actinium, also were shown to be fissionable with fast neutrons; and other particles, such as fast protons, deuterons, and alphas, along with gamma rays, proved to be effective in inducing the nuclear reactions.

1.3 Nuclear Fission

In nuclear physics, nuclear fission is a nuclear reaction in which the nucleus of an atom splits into smaller parts, often producing free neutrons and lighter nuclei, which may

eventually produce photons (in the form of gamma rays). Fission of heavy elements is an exothermic reaction which can release large amounts of energy both as electromagnetic radiation and as kinetic energy of the fragment [5]. For fission to produce energy, the total binding energy of the resulting elements has to be higher than that of the starting element. Fission is a form of nuclear transmutation because the resulting fragments are not the same element as the original atom. The figure 1.2 shows the nuclear fission.

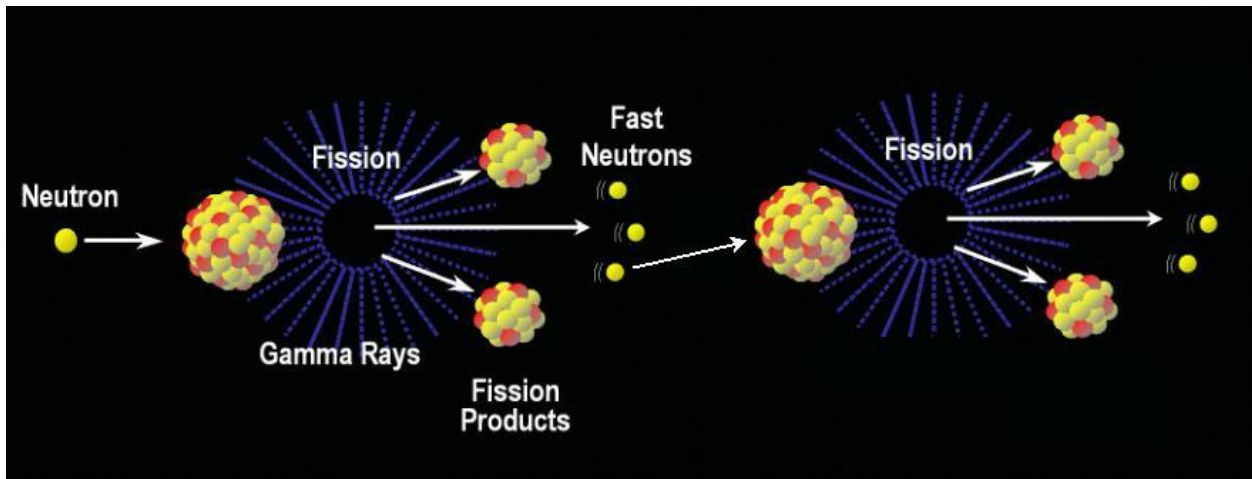
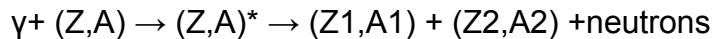


Figure1.3 Nuclear Fission Process

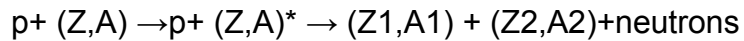
Nuclear fission can occur without neutron bombardment, as a type of radioactive decay. This type of fission is called the spontaneous fission and it is rare except in a few heavy isotopes. In nuclear reactions, a subatomic particle collides with an atomic nucleus and causes changes to it. Nuclear reactions are thus driven by the mechanics of bombardment, not by the relatively constant exponential decay and half-life characteristic of spontaneous radioactive processes.

For inducing fission, one has to provide energy to the nucleus, so that its parts can overcome the fission barrier, or form a compound nucleus where the barrier is diminished or eliminated

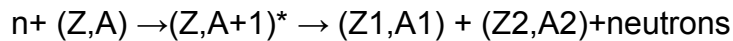
Photofission: In photofission high energy photons induce fission in the heavier elements



-proton induced fission



-neutron induced fission



1.4 Fission explained with the help of liquid drop model

Fission process can be explained with help of liquid drop model. The incident neutron combines with the nucleus to form highly energetic compound nucleus. Its extra energy is partly the kinetic energy of the neutron but largely the added binding energy of the incident neutron. This energy appears to initiate a series of rapid oscillations in the drop, which tend to distort the spherical shape so that the drop may become ellipsoidal in shape. The surface tension forces tend to make the drop return to its original spherical shape, while the excitation energy tends to distort the shape still further. If the excitation energy is sufficiently large, the drop may attain the shape of a dumb-bell. Thus, there is a threshold energy required to distort the nucleus so that the nucleus cannot return to its initial stage. When the distortion produced is not pronounced enough to get the nucleus beyond the critical point, the ellipsoid will return to the spherical shape with the excitation energy being liberated in the form of γ -rays and we have a radiative capture rather than fission.

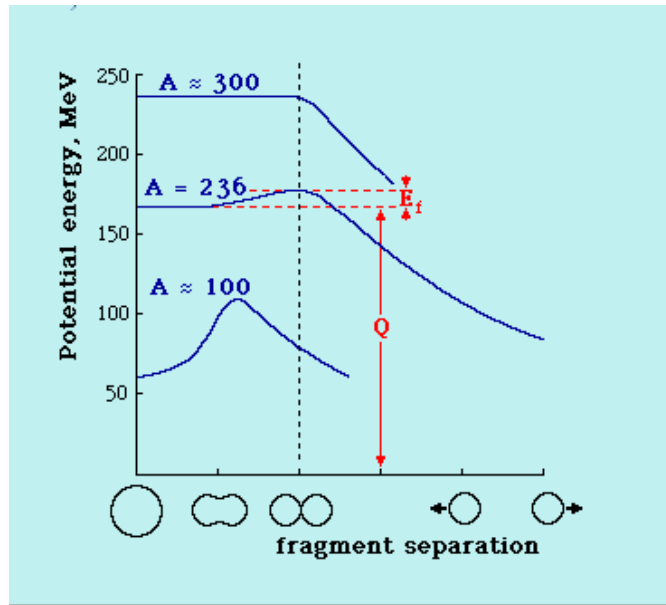


Figure 1.4 Potential barrier and Compound nucleus formation

The figure 1.3 shows schematically the shape of the barrier as a function of the deformation or fragment separation for different values of the atomic mass number (A). A great many nuclear reactions are known. Nuclear fission differs importantly from other types of nuclear reactions in that it can be amplified and sometimes controlled via a nuclear chain reaction. In such a reaction, free neutrons released by each fission event can trigger yet more events, which in turn release more neutrons and cause more fission.

The chemical element isotopes that can sustain a fission chain reaction are called nuclear fuels, and are said to be fissile. The most common nuclear fuels are ^{235}U and ^{239}Pu (the isotope of plutonium with an atomic mass of 239). These fuels break apart into a bimodal range of chemical elements with atomic masses centering near 95 and 135 u (fission products). In a nuclear reactor or nuclear weapon, the overwhelming majority of fission events are induced by bombardment with another particle, a neutron, which is itself produced by prior fission events.

A nuclear chain reaction occurs when one nuclear reaction causes an average of one or more nuclear reactions, thus leading to a self-propagating number of these reactions. Several heavy elements, such as uranium, thorium, and plutonium, undergo both

spontaneous fission, a form of radioactive decay and induced fission, a form of nuclear reaction. Elemental isotopes that undergo induced fission when hit by a free neutron are called fissionable and the isotopes that undergo fission when hit by a thermal, slow moving neutron are also called fissile. A few particularly fissile and readily obtainable isotopes (^{235}U and ^{239}Pu) are called nuclear fuels because they can sustain a chain reaction and can be obtained in large enough quantities to be useful. All fissionable and fissile isotopes undergo a small amount of spontaneous fission which releases a few free neutrons into any sample of nuclear fuel. Such neutrons would escape rapidly from the fuel and become a free neutron, with a half-life of about 15 minutes before they decayed to protons and beta particles.

Not all fissionable isotopes can sustain a chain reaction. For example, ^{238}U , the most abundant form of uranium, is fissionable but not fissile. It undergoes induced fission when impacted by an energetic neutron with 1 MeV of kinetic energy. There are few neutrons produced by ^{238}U fission are energetic enough to induce further fissions in ^{238}U , so no chain reaction is possible with this isotope. Instead, bombarding ^{238}U with slow neutrons causes it to absorb them (becoming ^{239}U) and decay by beta emission to ^{239}Np which then decays again by the same process to ^{239}Pu . That process is used to manufacture ^{239}Pu in breeder reactors. Since plutonium-239 is also a fissile element which serves as fuel.

Fissionable, non-fissile isotopes can be used as fission energy source even without a chain reaction. Bombarding ^{238}U with fast neutrons induces fissions, releasing energy as long as the external neutron source is present. This is an important effect in all reactors where fast neutrons from the fissile isotope can cause the fission of nearby ^{238}U nuclei, which means that some small part of the ^{238}U is "burned-up" in all nuclear fuels, especially in fast breeder reactors that operate with higher-energy neutrons.

1.5 Energy released in Nuclear Fission

The typical fission events release about two hundred MeV of energy for each fission event. The chemical oxidation reactions (such as burning coal or TNT) release at most a few eV per event, so nuclear fuel contains at least ten million times more usable

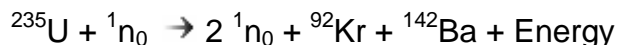
energy than does chemical fuel. The energy of nuclear fission is released as kinetic energy of the fission products and fragments, and as electromagnetic radiation in the form of gamma rays. In a nuclear reactor, the energy is converted to heat as the particles and gamma rays collide with the atoms that make up the reactor and its working fluid is usually water or occasionally heavy water.

When a uranium nucleus fissions into two daughter nuclei fragments, an energy of ~200 MeV is released. For uranium-235 (total mean fission energy 202.5 MeV), typically ~169 MeV appears as the kinetic energy of the daughter nuclei, which fly apart at about 3% of the speed of light, due to Coulomb repulsion. Also, an average of 2.5 neutrons are emitted with a kinetic energy of ~2 MeV each (total of 4.8 MeV). The fission reaction also releases ~7 MeV in prompt gamma ray photons.

This energy amounts to about 181 MeV, or ~ 89% of the total energy. The remaining ~ 11% is released in beta decays which have various half-lives, but begin as a process in the fission products immediately and in delayed gamma emissions associated with these beta decays. For example, in uranium-235 this delayed energy is divided into about 6.5 MeV in betas, 8.8 MeV in antineutrinos (released at the same time as the betas), and finally, an additional 6.3 MeV in delayed gamma emission from the excited beta-decay products (for a mean total of ~10 gamma ray emissions per fission, in all).

Now the important point which comes in mind is that, from where does this huge amount of energy comes?

In the section above we described what happens when a ^{235}U atom fissions. One can consider the following equation as an example:



The mass seems to be the same on both sides of the reaction. So it becomes a puzzle to resolve the source of this energy. In other words, it seems that no mass is converted into energy. However, this is not entirely correct [6]. The mass of an atom is more than the sum of the individual masses of its protons and neutrons, which is what those numbers represent. Extra mass is a result of the binding energy that holds the protons

and neutrons of the nucleus together. Thus, when the uranium atom is split, some of the energy that held it together is released as radiation in the form of heat. Because energy and mass are one and the same, the energy released is also mass released. Therefore, the total mass does decrease a tiny bit during the reaction.

1.6 Compound nucleus formation and its decay

When a projectile and target come into close contact during a nuclear reaction they form a combined system in which the nucleons interact strongly with each other. Expect when this intermediate system is light, the energy carried in from the entrance channel is usually not invested in one or a few degrees of freedom, i.e. in single particle or collective excitations (this would correspond to direct processes) but is shared more or less stochastically among many complicated configurations. Once this happens, it takes a long time on a nuclear scale until the energy is concentrated again in some configuration of nucleons from which a transition to an open final channel can take place [7].

1.6.1 Compound nucleus mechanism

It was Neil Bohr (1936) who found a suitable approach to the theory of such reactions by introducing the concept of a compound nucleus. In compound nucleus mechanism there are two steps:

- (1) In first step, the incident particle is absorbed by the nucleus, forming an intermediate stage called compound nucleus which remains for a long time ($\sim 10^{-16}$ sec). During this time the kinetic energy of the incident particle is shared among all the nucleons. All memory of the incident particle and the target is lost. The compound formed is always in a highly excited unstable state. At this stage the statistical equilibrium is reached and the average number of excited degrees of freedom becomes constant.
- (2) In the second step, the emission takes place through statistical fluctuations from the equilibrium, through the exit channels. This may be understood as a statistical evaporation of nucleons or light particles. The angular distributions

of compound nucleus reactions are completely isotropic or symmetric about 90° in the C-M frame.

The compound nucleus is highly excited. It also carries an angular momentum equal to the sum of the angular momentum of the relative motion in the entrance channel and the spins of the initial collision partners. The excitation energy and the angular momentum of the compound nucleus are eventually released via decay into smaller fragments. For compound nuclei at energies corresponding to incident laboratory energies $E < 10$ MeV per nucleon of the fusing projectile (these are the energies in which we are mainly interested in the following discussion) we distinguish two main decay schemes :

Evaporation, i.e. emission of light particles like neutrons, protons, α -particles and so on. There remains a bound residual nucleus called evaporation residue of a slightly lower mass than the compound nucleus. The particle evaporation process is generally accompanied by γ -emission, which has to be taken into account in the energy and angular momentum balance. The evaporation residue contains all the nucleons originally present in the compound nucleus except the few evaporated ones.

Fission: where the compound nucleus splits into two halves of more or less equal size. This process is accompanied by evaporation of light particles out of the fissioning nucleus, and similarly the fission fragments will generally decay further by evaporation. The emitted particles are called pre-scission and post-scission particles, respectively.

1.7 Non-compound Nucleus

However depending on the reaction conditions and energies involved, one may observe other competing decay probabilities where compound nucleus formation does not take place. Such decays are called non compound nucleus decays. The incomplete fission (ICF), Deep inelastic collisions (DIC) and Quasi fission (QF) etc fall in this category. In recent times lot of work has been done to access the NCN contribution in the decay of heavy ions formed in different mass regions.

For lighter systems evaporation predominates. The rate of production of evaporation residues is then a measure of the fusion cross section (fusion- evaporation). For medium-heavy systems evaporation components competes with the fission process. For heavy systems fission is the dominant mode of decay of the compound nucleus. For highly fissile systems, the fusion cross section is generally determined by the fission cross section (fusion-fission), as the evaporation residue or other competing NCN components are negligible small.

In general it is the sum of the measured cross sections for these two main modes of decay i.e. ER and Fission which yields the magnitude of the fusion cross section. In order to verify that a compound nucleus has indeed been formed in the process, further evidence (relating to the momenta of the evaporation residues, the angular distribution of the emitted particles, or the angle between the fission fragments) must be added to identify a given reaction as a compound reaction. At projectile energies $E \sim 10$ MeV per nucleon incomplete fusion starts to compete with complete fusion, i.e. processes like pre-equilibrium particle emission and projectile break-up occur which lead to an incomplete transfer of linear momentum.

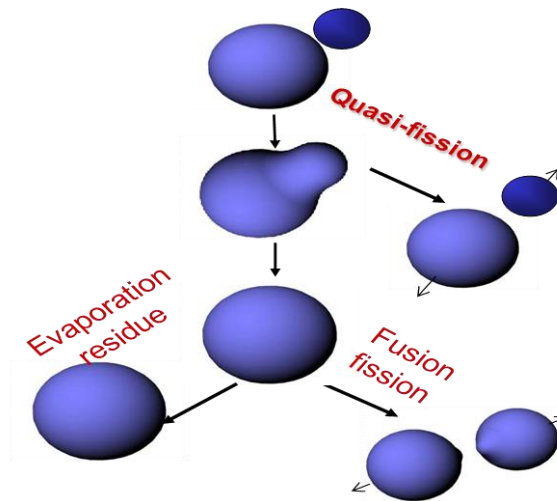


Figure 1.5 Competing decay processes[8]

It is relevant to mention here that the presence of non compound nucleus decay gives rise to a phenomenon known as Fusion hindrance as the compound nucleus formation is denied at the cost of NCN decay. This kind of fusion hindrance has been observed in the decay of majority of pre-actinide nuclear systems. It may be noted that concept of fusion hindrance or barrier modification can be addressed via neck length parameter (ΔR), the only parameter of DCM (discussed in chapter 2). This feature of DCM beside its utility related to prediction of ER, fission and NCN component in different mass region, put it in the selected list of models regarding nuclear dynamics and nuclear structure investigation.

1.8 Fusion hindrance in heavy elements

The Synthesis of a super-heavy element (SHE), which is made by heavy ion fusion reactions, is an important and exciting issue for nuclear physics [9] Because the decay properties of the SHE give information on the shell effects of nucleus, without which such a heavy nucleus could not exist due to overwhelming repulsive Coulomb force. It is generally accepted that the production of evaporation residues comprises of two separate processes, the fusion between two interacting nuclei (entrance channel) and the survival against fission in the course of the deexcitation process (exit channel). The former process is successfully described by a coupled channel model for projectile-target combinations with $Z_1 Z_2 \leq 1300$. On the other hand, in heavy systems ($Z_1 Z_2 > 1300$), the formation of a compound nucleus is hindered. This is caused by the friction generated between the interacting two nuclei in the course of fusion process. The friction force decreases the kinetic energy of the nuclei, which hinders a complete fusion. To drive the system to the compound nucleus, an additional bombarding energy is needed above the Coulomb barrier to compensate for the energy loss by friction, which is called extra-extra-push energy (*EXX*) [9]. Fusion hindrance may be related to the contact point of the interacting two nuclei relative to the fission saddle point of the compound nucleus, from the consideration that the necessary condition for forming a compound nucleus is the dynamical trajectory to pass inside the fission saddle point on the potential energy surface. Simple consideration for the fusion process using two spherical nuclei tells that the distance between mass centers at the contact point

expands for heavy systems, which would result in large fusion hindrance. However, even for systems having Z_1Z_2 values larger than 1300, the compact configuration may be achieved by using a prolately deformed target. So the Z_1Z_2 product need to be considered with caution depending on reaction condition and shape of nuclei involved in the reaction. Fusion hindrance in the pre-actinide region is currently an active area of investigation in the field of heavy ion reactions. Suppression in the evaporation residue cross section [10–14], anomalous fission fragment angular distribution [15–20], and broadening in the fission fragment mass distribution [21] are considered as signatures of fusion hindrance or NCN fission. Asymmetric fission due to the contribution from NCN fission has also been reported [22, 23]. In the present work we have studied the decay of a pre actinide nucleus ^{204}Po formed in $^{16}\text{O}+^{188}\text{Os}$ reaction. As Z_PZ_T is quite low for this reaction so it extends an ideal case to look out for non availability of non compound nucleus component in this reaction.

1.9 Stability of nucleus

The most important quantity determining the stability of a nucleus is its energy as compared to the energies of any two component nuclei into which it may be subdivided (we consider only the decomposition into two fragments; the stability against disintegration into more than two fragments is generally greater). It may be noted that more than two fragments can be formed in a nuclear reaction but generally it happens at larger value of incident energy.

Figure 1.5 shows schematically a nucleus A and its decomposition into two fragments A_1 and A_2 at contact. Because of the short range of the nuclear forces, we may assume that there is Coulomb repulsion but no nuclear attraction between the fragments in this configuration. If all systems are in their ground state, we have for the difference between the energy of the separated fragments (equal to the sum of the internal energies of the fragments (A_1, Z_1) and (A_2, Z_2) plus the coulomb energy V_C at contact) and the energy of the nucleus (A, Z) is

$$B = B(A_1, Z_1; A_2, Z_2) \\ = E(A_1, Z_1) + E(A_2, Z_2) + V_c(A_1, Z_1; A_2, Z_2) - E(A, Z)$$

where $A = A_1 + A_2$, $Z = Z_1 + Z_2$, $E(A_i, Z_i)$ is the internal energy of the nucleus (A_i, Z_i) and the coulomb energy of the fragments in contact at the radius R_C is given by $V_C(A_1, Z_1; A_2, Z_2) = Z_1 Z_2 e^2 / R_C$

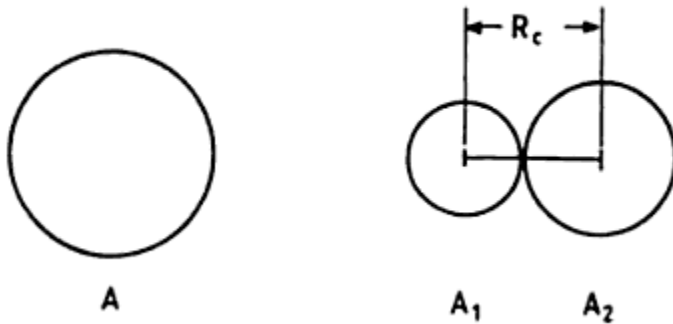


Fig. 1.5 Decomposition of a nucleus into two fragments

The quantity B is the energy released when the two fragments in contact from the nucleus (A, Z) , which we call the compound nucleus. Conversely, it is the internal energy above the ground state level which the compound must have in order to ascend the height B defined by the energy of the two decay products at contact as shown in fig. 1.6. For $B > 0$ the compound nucleus is stable and for $B < 0$, it is unstable

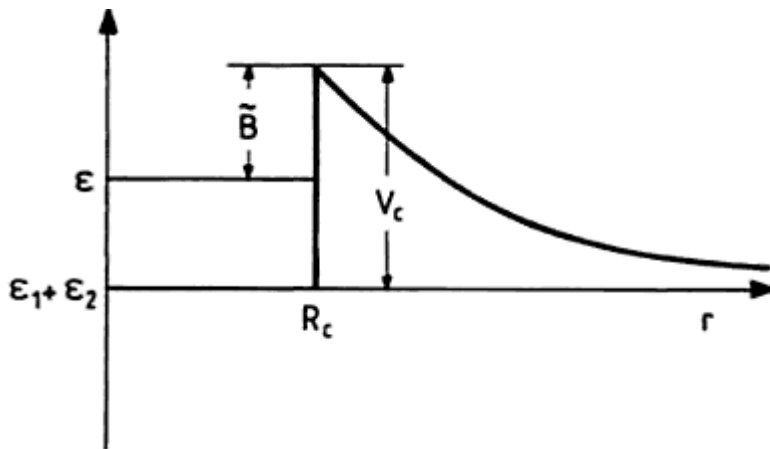


Fig. 1.6 Potential barrier as a function of relative separation between fragments

For the calculation of ground state energy $E(A, Z)$ one may use of Bethe-Weizsacker liquid drop formula in the form proposed by Myers and Swiatecki

$$\epsilon(A, Z) = \epsilon_V(A, Z) + \epsilon_S(A, Z) + \epsilon_C(A, Z).$$

Here we introduce the volume energy

$$\epsilon_V(A, Z) = - \left[1 - \kappa \left(\frac{N - Z}{A} \right)^2 \right] a_V A,$$

the surface energy

$$\epsilon_S(A, Z) = \left[1 - \kappa \left(\frac{N - Z}{A} \right)^2 \right] a_S A^{2/3}$$

and coulomb energy

$$\epsilon_C(A, Z) = \frac{3}{5} \frac{e^2 Z^2}{r_0 A^{1/3}} \left(1 - \frac{5}{6} \frac{\pi^2 a^2}{r_0^2 A^{2/3}} \right),$$

The coefficients in these equations have the values $a_V = 15.67$ MeV, $a_S = 18.56$ MeV, $r_0 = 1.204$ fm and $a = 0.546$ fm.

The energy released $B = B(A, Z, \alpha)$ or the energy needed for a split-up into a system of fragments $(A_1, A - A_1)$ (calculated from above equations for different compound nuclei i.e. for different values of A) as a function of the asymmetry parameter $\alpha = A_1/A$

The three regions of stability of compound nucleus can be distinguished

1. If $A > 120$, the value of $B(\alpha)$ is larger for $\alpha = 1/2$ and low for $\alpha \sim 0$; the decay to fragments with very different masses ($\alpha \ll 1$) are energetically favored. The daughter

nuclei are a light nucleus (n, p, α ,.....) and a heavy one with a mass slightly less than that of the mother nucleus. The light nucleus is called the evaporated particle and the heavy fragment, the evaporation residue. A compound reaction in which the compound nucleus decays in this very asymmetric fashion is called a fusion – evaporation reaction.

2. For $120 < A < 300$ symmetric final configurations are favoured. A compound reaction terminating in a near symmetric decay is called fusion-fission reaction.

3. For $A > 300$, the compound nucleus is unstable even in its ground state. In reactions where the value of total mass lies in this region the compound nucleus does not have the time to equilibrate so as to decay afterwards by the energetically favoured symmetric fission. Instead, the di-nuclear complex in the entrance channel immediately goes over into the final two- body configuration. One speaks here of a capture or fast fission process because the projectile is only captured briefly without forming a compound nucleus and the intermediary system decays more rapidly than in normal fission.

In this work we shall concentrate mainly on the issue of fission dynamics prevailing ER and fission. However a parallel interest will be explore the possibility of NCN component in decay of nucleus under investigation. Beside this, an effort will be made to look out for the possible role of deformation and orientations in the decay of nucleus formed in the region $A \sim 200$.

2.0 References:

- [1] <http://science.howstuffworks.com/manhattan-project1.htm>
- [2] <http://www.sciencelarified.com/mu-o/Nuclear-Fission.html>
- [3] <http://www.britannica.com/EBchecked/topic/421629/nuclear-fission>
- [4] <http://science.jrank.org/pages/47191/Nuclear-Fission-History.html>
- [5] <http://en.wikipedia.org/wiki/Nuclear-Fission>
- [6] <http://library.thinkquest.org/17940/texts/fission/fission.html>
- [7] <http://books.google.co.in/books?id=SO4Lmw8XoEMC&pg=PA123&lpg=PA123>
- [8] www.cnr09.com/pres/jeudi_session1/banerjee.ppt
- [9] <http://wwwsoc.nii.ac.jp/jnrs/paper/JN31/20.pdf>
- [10] K. Nishio *et al.*, Eur. Phys. J. A 29, 281 (2006).
- [11] S. Mitsuoka, H. Ikezoe, K. Nishio, K. Satou, and J. Lu, Phys. Rev. C 65, 054608 (2002).
- [12] K. Nishio, H. Ikezoe, Y. Nagame, M. Asai, K. Tsukada, S. Mitsuoka, K. Tsuruta, K. Satou, C. J. Lin, and T. Ohsawa, Phys. Rev. Lett. 93, 162701 (2004).
- [13] R. N. Sagaidak *et al.*, Phys. Rev. C 68, 014603 (2003).
- [14] M. Trotta *et al.*, Nucl. Phys. A787, 134 (2007).
- [15] J. P. Lestone, A. A. Sonzogni, M. P. Kelly, and R. Vandenbosch, Phys. Rev. C 56, R2907 (1997)
- [16] Bhivash R. Behera *et al.*, Phys. Rev. C 69, 064603 (2004).

- [17] G. N. Knyazheva *et al.*, Phys. Rev. C 75, 064602 (2007).
- [18] R. Tripathi, K. Sudarshan, S. Sodaye, S. K. Sharma, and A. V. R. Reddy, Phys. Rev. C 75, 024609 (2007).
- [19] B. B. Back, R. R. Betts, J. E. Gindler, B. D. Wilkins, S. Saini, M. B. Tsang, C. K. Gelbke, W. G. Lynch, M. A. McMahan, and P. A. Baisden, Phys. Rev. C 32, 195 (1985).
- [20] R. Tripathi, K. Sudarshan, S. Sodaye, A.V.R.Reddy, K. Mahata, and A. Goswami, Phys. Rev. C **71**, 044616 (2005).
- [21] R. Rafiei *et al.*, Phys. Rev. C 77, 024606 (2008).
- [22] E. V. Prokhorova *et al.*, Nucl. Phys. **A802**, 45 (2008).
- [23] K. Nishio, H. Ikezoe, S. Mitsuoka, I. Nishinaka, Y. Nagame, Y. Watanabe, T. Ohtsuki, K. Hirose, and S. Hofmann, Phys. Rev. C **77**, 064607 (2008).

CHAPTER 2

METHODOLOGY

DYNAMICAL CLUSTER DECAY MODEL

The dynamical cluster-decay model (DCM) is developed for the decay of hot and rotating compound nuclei (CN) formed in low-energy heavy-ion reactions. The model is a non-statistical description for the decay of a compound nucleus (CN) to light particles, intermediate mass fragments, fusion-fission and quasi-fission (equivalently, capture) processes. The quasi-fission or capture is the non-compound nucleus contribution, determined empirically. The deformations and orientation degrees of freedom (for compact orientations) of the incoming nuclei and of out-going nuclei/fragments are also included.

The model is worked out in terms of only one parameter, namely the neck-length parameter, which is related to the total kinetic energy TKE (T) or effective Q value $Q_{\text{eff}}(T)$ at temperature T of the hot CN and is defined in terms of the CN binding energy and ground-state binding energies of the emitted fragments. The emission of both the light particles (LP), with $A \leq 4$, $Z \leq 2$, as well as the complex intermediate mass fragments (IMF), with $4 < A < 20$, $Z > 2$, is considered as the dynamical collective mass motion of preformed clusters through the barrier.

2.1 Introduction

A comprehensive study of various types of emission from the ground state as well as excited states of compound nucleus (CN) formed in low energy reaction is important, as it gives information about the nuclear structure aside the underlying nuclear forces. At low energies and average nuclear force field acts between decaying fragments which in turns ensure possibility of more than one decay path. This average nuclear force field is largely influenced by entrance channel, angular momentum and the temperature consideration along with contribution of deformed and orientation effects. An extensive study of these nuclear properties lead to a better understanding of reaction dynamics of rare nuclear species that make the unexplored part of the nuclear chart, called exotic nuclei.

The main aim of the work is to study heavy ion reaction dynamics especially the decay of excited compound nucleus using the dynamical cluster decay model(DCM) [1]-[9].It is important to note that deformation and orientation effects of the reaction partner and decay products are explicitly included along with temperature and angular momentum contribution in this model. The ground state cluster decay of radioactive nuclei have also been undertaken with in the preformed cluster decay model [10]-[18].Again having deformation and orientation effects of the cluster as well as daughter nuclei included in it.

This model is a two step model

(a) First step is quantum mechanical preformation probability P_0 of the decay products or cluster formed in the mother nuclei

(b)Second step is the penetration of the fragments/ clusters through the interaction barrier

The P_0 based on QMFT is also discussed here in section 2.5. Penetration probability P is given in section 2.6. These two crucial parameters (P_0 and P) have been developed and used [9],[17],[18],[22],[23], to incorporate the deformation effects of oriented nuclei. The assault frequency, ν_0 with which the preformed cluster tries to tunnel the barrier in the ground state decay is discussed in section 2.7

2.2 The Dynamical Cluster Decay Model (DCM)

For Hot and Rotating Compound Nucleus

The dynamical cluster decay model (DCM) [1]-[9] for hot and rotating nuclei (i.e. angular momentum and temperature both not equal to zero) is a reformation of the preformed cluster model of Gupta and collaborators for ground state decay ($\ell =0,t=0$) in cluster radioactive (CR) and related phenomena [10]-[18] like PCM, DCM is also based upon the dynamical (or quantum mechanical) fragmentation theory of cold phenomena in heavy ion reaction and fission dynamics. In DCM, besides the temperature and angular

momentum effects in the decay of excited compound nuclei, the deformation and orientation effect of the decay products are also taken care, especially in the decay of heavy excited CN for which the deformation of the decay product seems to play significant role. The DCM, worked out in terms of the collective coordinates of mass asymmetry $\eta = \frac{A_1 - A_2}{A_1 + A_2}$ and relative separation R respectively gives

- (i). The nucleon-division (or exchange) between the outgoing fragments, and
- (ii). The transfer of kinetic energy of incident channel (E_{cm}) to internal excitation (total excitation or total kinetic energy ,TXE or TKE) of the outgoing channel. It may be noted that the fixed decay point $R = R_a$ (defined later), at which the process is calculated depends upon temperature T as well as on η (i.e. $R(T, \eta)$). This energy transfer process can be calculated as follows with the help of Fig 2.1

$$E_{CN}^* = E_{c.m} + Q_{in} = |Q_{out}| + TKE(T) + TXE(T) \quad (2.1)$$

The CN excitation E_{CN}^* is related to temperature T (in MeV) and is given by

$$E_{CN}^* = \frac{1}{9}AT^2 - T(Mev) .$$

Using the decoupled approximation to R and η -motions, the DCM define the decay cross section ,in terms of partial waves, as[3]-[9] ;

$$k = \sqrt{\frac{(2\mu E_{c.m})}{\hbar^2}} ; \sigma = \sum_{l=0}^{l_c} \sigma_l = \frac{\pi}{k^2} \sum_{l=0}^{l_c} (2l + 1) P_0 P \quad (2.2)$$

Where P_0 the preformation probability refers to η -motion and P, the penetrability to the R- motion, discussed in section 2.3.7 and 2.4 respectively. Here the complex fragments (both light and heavy fragments) are treated as the dynamical collective mass motion of preformed cluster or fragments through the barrier .The structure information of the CN enters the model via preformation probability P_0 (also known as spectroscopic factor) of the fragments given by the solution of stationary Schrödinger equation in η at the

fixed $R=R_a$, the first turning point of the penetrability path shown in figure 2.1 for the different ℓ -values.

$$\left\{ -\frac{\hbar^2}{2\sqrt{B_{\eta\eta}}} \frac{\partial}{\partial \eta} \frac{1}{\sqrt{B_{\eta\eta}}} \frac{\partial}{\partial \eta} + V_R(\eta, T) \right\} \psi^\nu(\eta) = E^\nu \psi^\nu(\eta) \quad (2.3)$$

with $\nu=0,1,2,3,\dots$ referring to the ground state and excited state solution .

2.2.1 Postulate of first turning point

For the decay of the hot compound nucleus, we use the postulate of first turning point

$$R_a = R_t + \Delta R(T) \quad (2.4)$$

Where

$$R_t = R_1 + R_2 \quad (2.5)$$

$\Delta R(T)$ is the neck length parameter that assimilates the neck formation effects. This method is introducing a neck length parameter similar to that used in scission point [24] and saddle point [25-26] statistical fission model. The R_i are radius vectors which are also made temperature dependent can be calculated as

$$R_i(\alpha_i) = R_{0i} \left[1 + \sum_{\lambda} \beta_{\lambda i} Y_{\lambda}^{(0)}(\alpha_i) \right] \quad (2.6)$$

with

$$R_{0i}(T) = 1.28 A_i^{1/3} - 0.76 + 0.8 A_i^{-1/3} \times (1 + 0.0007 T^2), \quad (2.7)$$

The corresponding potential $V(R_a)$ acts like an effective Q-value, Q_{eff} , for the decay of the hot CN at temperature T , to two exit-channel fragments observed *ing.s.* ($T=0$), defined by

$$\begin{aligned} Q_{\text{eff}}(T) &= B(T) - [B_L(T=0) + B_H(T=0)] \\ &= \text{TKE}(T) = V(R_a(T)) \end{aligned} \quad (2.8)$$

with B's as the respective binding energies.

The above defined decay of a hot CN into two cold ($T=0$) fragments, via Eq. (2.8), could apparently be achieved only by emitting some light particles (LPs), like n , p , α , or γ -rays of energy

By defining $Q_{\text{eff}}(T)$ as in Eq. (2.8), in this model we treat the LP emission at par with the heavy fragments, called intermediate mass fragments (IMFs) emission. Thus, in this model a non-statistical dynamical treatment is attempted for not only the emission of IMFs but also of multiple LPs, understood so-far only as the statistically evaporated particles in a CN emission. It may be reminded here that the statistical model (CN emission) interpretation of IMFs is not as good as it is for the LP production [24–29].

2.2.2 The second turning point

In terms of $Q_{\text{eff}}(T)$, the second turning R_b satisfies (see Fig. 2.1)

$$V(R_a, l) = V(R_b, l) = Q_{\text{eff}}(T, l) = \text{TKE}(T). \quad (2.9)$$

with the l -dependence of R_a defined by

$$V(R_a, l) = Q_{\text{eff}}(T, l = 0), \quad (2.10)$$

which means that the R_a , given by Eq. (2.4), is the same for all l -values, and that $V(R_a, l)$ acts like an effective Q-value, $Q_{\text{eff}}(T, l)$, given by the total kinetic energy $\text{TKE}(T)$. Then, using (2.9), $R_b(l)$ is given by the l -dependent scattering potentials, at fixed T as

$$\begin{aligned} V(R, T, l) = & V_c(Z_i, \beta_{\lambda_i}, \theta_i, T) + V_p(A_i, \beta_{\lambda_i}, \theta_i, T) \\ & + V_t(R, A_i, \beta_{\lambda_i}, \theta_i, T) \end{aligned} \quad (2.11)$$

which is normalized to the exit channel binding energy $B_L(T) + B_H(T)$. Such a potential is illustrated in Fig. 2.1, $^{16}\text{O} + ^{188}\text{Os} \rightarrow ^{204}\text{Po}$ at $l = 0$ value. The second turning point R_b is marked for the $l = 0\hbar$ case of $R_a = R_t + \Delta R(T)$. The decay path for the l -values begins at $R = R_a$.

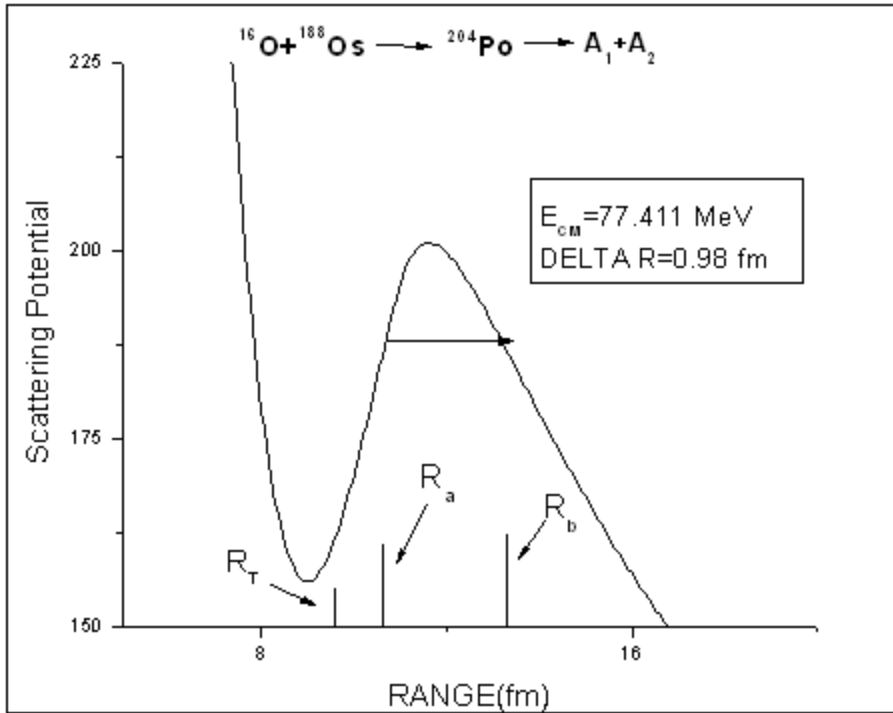


Fig.2.1. Scattering Plot for $^{16}\text{O} + ^{188}\text{Os} \rightarrow ^{204}\text{Po}$ reaction

The collective fragmentation potential $V(R, \eta, T)$ in Eq. (2.11) is calculated according to the Strutinsky method by using the T-dependent liquid drop model energy V_{LDM} of [30], with its constants at $T=0$ re-fitted [3, 4] to give the recent experimental binding energies given by [31], and again refitted [9] to give the recent experimental binding energies [32] and calculate binding energies [33] (only for those nuclides for which experimental data is not available. the “empirical” shell corrections δU are of Ref. [34] (In the Appendix of [3] and Eq. (8) of [4], $a_a=0.5$, instead of unity). Then, including the T-dependence also in Coulomb, nuclear proximity, and l -dependent potential in complete sticking limit of moment of inertia, we get

$$V(R, \eta, T) = \sum_{i=1}^2 [V_{LDM}(A_i, Z_i, T) + \sum_{i=1}^2 [\delta U_i] \exp\left(\frac{-T^2}{T_0^2}\right) + V_c(Z_i, \beta_{\lambda_i}, \theta_i, T) + V_p(A_i, \beta_{\lambda_i}, \theta_i, T) + V_l(R, \beta_{\lambda_i}, \theta_i, T) \quad (2.12)$$

where the T-dependent terms V_c , V_p and V_l are defined as follows.

2.3 Overview of potentials

2.3.1 The proximity potential:-

When two surfaces approach each other within a small distance of less than $\sim 2\text{fm}$, comparable with the surface thickness of interacting nuclei, or when a nucleus is at the verge of dividing into two fragments, then the two surfaces actually face each other across a small gap or crevice. In both cases, the surface energy term alone could not give rise to the strong attraction that is observed when the two surfaces are brought in close proximity. Such additional attractive forces are called proximity forces and the additional potential due to these forces is called the nuclear proximity potential. The proximity potential for hot deformed nuclei is [33-34] (see section 2.3.3)

$$V_p(A_i, \beta_{\lambda_i}, \theta_i, T) = 4\pi\bar{R}(T)\gamma b(T)\Phi(s_0(T)) \quad (2.13)$$

2.3.2 The Coulomb potential

Coulomb potential describes the force of repulsion between two interacting nuclei due to their charges. It acts along the line joining the two nuclei. The Coulomb potential for two interacting spherical nuclei is given as

$$V_c = Z_1 Z_2 e^2 / R \quad (2.14)$$

For interacting deformed and oriented nuclei, different authors [19-21] have derived it differently. In this thesis work, we have started with Coulomb potential of Wong [21], given for two non-overlapping charge distributions, having quadrupole deformations only, i.e.,

$$V_c = \frac{Z_1 Z_2 e^2}{R} + \left(\frac{9}{20\pi} \right)^{1/2} \left(\frac{Z_1 Z_2 e^2}{R^3} \right) \sum_{i=1}^2 R_i^2(\alpha_i) \beta_{2i} P_2(\cos\theta_i) + \left(\frac{3}{7\pi} \right) \left(\frac{Z_1 Z_2 e^2}{R^3} \right) \sum_{i=1}^2 R_i^2(\alpha_i) \left[\beta_{2i} P_2(\cos\theta_i) \right]^2 \quad (2.15)$$

In this expression, the quadrupole-quadrupole interaction term, proportional to $\beta_{21}\beta_{22}$, is neglected since it has a short-range character. For nuclei lying in the same plane we have generalized it to include the higher order deformations ($\lambda = 3, 4\dots$), obtaining

$$V_c(Z_i, \beta_{\lambda i}, \theta_i, T) = \frac{Z_1 Z_2 e^2}{R(T)} + 3Z_1 Z_2 e^2 \sum_{i,i=1,2} \frac{R_i^\lambda(\alpha_i, T)}{(2\lambda+1)R(T)^{\lambda+1}} Y_\lambda^{(0)}(\theta_i) \left[\beta_{\lambda i} + \beta_{\lambda i}^2 Y_\lambda^{(0)}(\theta_i) \right] \quad (2.16)$$

With R_i from eq (2.32) $Y_\lambda^{(0)}(\theta_i)$ are the spherical harmonic function with the radius vector given by Eq. (2.6) and surface thickness parameter

$$b(T) = 0.99(1 + 0.009T^2). \quad (2.17)$$

2.3.3 The angular momentum potential

$$V_l(R, A_i, \beta_{\lambda i}, \theta_i, T) = \frac{\hbar^2 l(l+1)}{2I_s(T)} \quad (2.18)$$

with the moment-of-inertia,

$$I_s(T) = \mu R^2 + \frac{2}{5} A_1 m R_1^2(\alpha_1, T) + \frac{2}{5} A_2 m R_2^2(\alpha_2, T).$$

Further, in Eq. (2.12), within the Strutinsky renormalization procedure, we have defined the binding energy B of a nucleus at temperature T as the sum of liquid drop energy $V_{LDM}(T)$ and shell correction $\delta U(T)$ i.e.

$$B(T) = V_{LDM}(T) + \delta U \exp\left(\frac{-T^2}{T_0^2}\right) \quad (2.19)$$

The T dependent liquid drop part of the binding energy VLDM(T) is from Davidson et al. [30], based on the semi-empirical mass formula of Seeger [35]. For the shell correction δU in Eq. (2.19), since there is no microscopic shell model known that gives the shell corrections for light nuclei, we use the empirical formula of Myers and Swiatecki [34].

The mass parameters $B_{\eta\eta}(\eta)$, representing the kinetic energy part in Eq. (2.3), are the smooth classical hydro-dynamical masses [36], for $\vartheta_1 = \vartheta_2 = 0^0$ and R_i taken as temperature dependent.

Finally, the l_c -value in Eq. (2.6) is the critical l -value, in terms of the bombarding energy $E_{c.m.}$. The reduced mass μ and the first turning point R_a of the entrance channel η_{in} , given by

$$l_c = R_a \sqrt{2\mu[E_{c.m.} - V(R_a, \eta_{in}, l = 0)]} / \hbar \quad (2.20)$$

or, alternatively, it could be fixed for the vanishing of fusion barrier of the incoming channel, called l_{fus} , or else the l -value (l_{max}) where the light-particle cross section $\sigma_{LP} \rightarrow 0$. This, however, could also be taken as a variable parameter [25, 37].

2.4 Classical Hydrodynamical Mass Parameters

The kinetic energy part of the Hamiltonian enters through the mass parameters. We use here the classical mass parameters of Kroger and Scheid [36]. The model of Kroger and Scheid is based on the hydro-dynamical flow, as shown in Fig. 2.2. This model gives a simple analytical expression, whose predictions are shown to compare nicely with the microscopic cranking model calculations. For the $B_{\eta\eta}$ mass we get

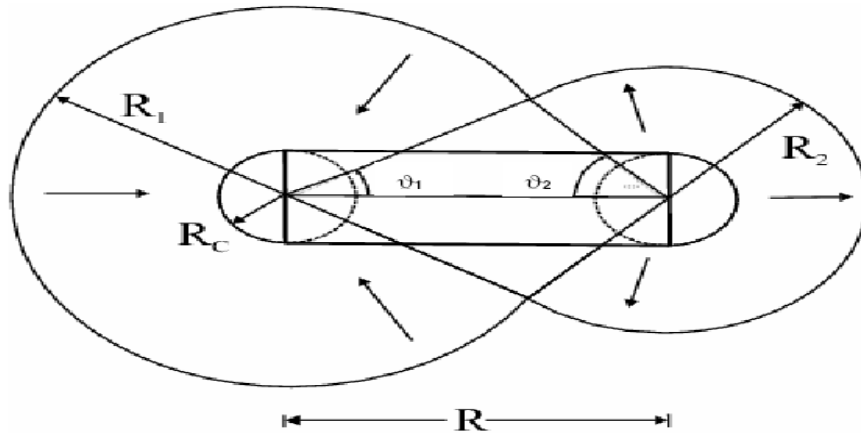


Fig.2.2. The geometry of classical hydrodynamical model for calculating mass parameter $B_{\eta\eta}$

$$B_{\eta\eta} = \frac{AmR^2}{4} \left[\frac{vt(1+\gamma)}{v_c \left(1 + \frac{vt(1+\gamma)}{v_c(1+\delta_2)} \right)} - 1 \right] \quad (2.21)$$

$$\text{With } \gamma = \frac{R_c}{2R} \left[\frac{1}{1 + \cos \vartheta_1} \left(1 - \frac{R_c}{R_1} \right) + \frac{1}{1 + \cos \vartheta_2} \left(1 - \frac{R_c}{R_2} \right) \right] \quad (2.22)$$

$$\delta = \frac{1}{2R} [(1 - \cos \vartheta_1) + (1 - \cos \vartheta_2)] \quad (2.23)$$

$$v_c = \pi^2 R_c^2 R \quad (2.24)$$

and $v_t = v_1 + v_2$, is the total conserved volume. The angles ϑ_1 and ϑ_2 and geometry of the model are shown in Fig. 2.3. For $\vartheta_1 = \vartheta_2 = 0$, $\delta = 0$ which corresponds to two touching spheres. R_c (is not equal to 0) is the radius of a cylinder of length R , having a homogeneous flow in it; whose existence is assumed for the mass transfer between the two spherical fragments. We have generalized this formalism for deformed nuclei by using the radii R_1 and R_2 for deformed nuclei.

2.5 Preformation Probability P_0

Once the Hamiltonian Eq. (2.25) is established, the Schrödinger equation in mass fragmentation co-ordinate η can be solved. On solving Schrodinger wave equation numerically, $|\psi^\nu(\eta)|^2$ gives the probability P_0 of finding the mass fragmentation η at a fixed R on the decay path.

$$P_0(A_2) = |\psi^\nu(A_2)|^2 \quad (2.25)$$

For fission studies, like the spontaneous fission and fission through the barrier, the motion in R at the saddle point is adiabatically slow as compared to the η motion. Therefore, the potential is minimized in the neck and deformation coordinates β_1 and β_2 at each R and η values. Starting from the nuclear ground state in spontaneous fission or cluster decay, and to have complete adiabaticity, only the lowest vibrational state $\nu = 0$ is occupied. Then, the mass (or charge) distribution yield, proportional to the probability

$|\psi^{(0)}(\eta)|^2$ or $|\psi^{(0)}(\eta_Z)|^2$ of finding a certain mass (or charge) fragmentation η (or ηZ) at a position R on the decay path, when scaled to, say, mass A_2 of one of the fragments ($d\eta = 2/A$) is given by:

$$Y(A_2) = |\psi_R^{(0)}(A_2)|^2 \frac{2}{A} \sqrt{B_{\eta\eta}(A_2)}. \quad (2.26)$$

However, if the system is excited or we allow interaction between various degrees of freedom, higher values of ν would also contribute. These enter via the excitation of higher vibrational states, and through the temperature dependent potential V and masses B_{ij} . The effect of adding temperature on potential V and masses B_{ij} is to reduce the shell effects in them, resulting finally in the liquid drop potential VLDM and smoothed (averaged) masses B_{ij} for the systems to be very hot. Apparently, cold fission means taking both the potential V and masses B_{ij} with full shell effects included in them and hot fission means using the VLDM and smoothed (averaged) masses B_{ij} . The possible consequence of such excitations are included here by assuming a Boltzmann like occupation of excited states

$$|\psi(\eta)|^2 = \sum_{\nu=0}^{\infty} |\psi^{\nu}(\eta)|^2 \exp\left(-\frac{E_{\nu}}{T}\right) \quad (2.27)$$

Note that we are dealing here with a directly measurable quantity, the mass (or charge) asymmetry, which works dynamically as mass (or charge) transfer coordinate. Thus, the calculated yields $Y(A_i)$ (or $Y(Z_i)$) are directly comparable with experiments. It may be stressed that there is no free parameter in these calculations. The nuclear shape, once minimized in the neck and deformation coordinates β_1 and β_2 at a given R ($=R_{\text{saddle}}$), remains fixed for both the mass and charge distributions of fission or decay fragments.

2.6 Penetration Probability P

Penetrability P measures the capability of fragments nucleus to penetrate the potential barrier generalized during compound nucleus formation.

2.7 Assault Frequency ν_0

For the cluster decay studies in the following section, another quantity of interest is the assault frequency ν_0 defined as, E_2

$$\nu_0 = \frac{v}{R_0} = \frac{\sqrt{(2E_2/\mu)}}{R_0} \quad (2.28)$$

where R_0 is the radius of parent nucleus and $E_2 = 1/2\mu v^2$ is the kinetic energy of the emitted cluster. Since both the emitted cluster and the daughter nucleus are produced in the ground state, the entire positive Q-value is the total kinetic energy ($Q = E_1 + E_2$) available for the decay process, which is shared between two fragments, such that for the emitted cluster

$$E_2 = \left(\frac{A_1}{A}\right)Q \quad (2.29)$$

and, $E_1 = Q - E_2$ is the recoil energy of the daughter nucleus.

2.8 References

- [1] R.K. Gupta, M. Balasubramiam, C. Mazzocchi, M. La Commara, and W. Scheid, Phys. Rev. C 65, 024601 (2002).
- [2] M.K. Sharma, R.K. Gupta, and W. Scheid, J. Phys. G 26, L45 (2000).
- [3] R.K. Gupta, R. Kumar, N.K. Dhiman, M. Balasubramiam, W. Scheid, and C. Beck, Phys. Rev. C 68, 014610 (2003).
- [4] M. Balasubramiam, R. Kumar, R.K. Gupta, C. Beck, and W. Scheid, J. Phys. G 29, 2703 (2003); R.K. Gupta, M.K. Sharma and B. Singh, Phys. Rev. C-to be published
- [5] R.K. Gupta, M. Balasubramiam, R. Kumar, D. Singh, and C. Beck, Nucl. Phys. A 738, 479c (2004).
- [6] R.K. Gupta, M. Balasubramiam, R. Kumar, D. Singh, C. Beck, and W. Greiner, Phys. Rev. C 71, 014601 (2005).
- [7] B.B. Singh, M.K. Sharma, R.K. Gupta, and W. Greiner, Int. J. Mod. Phys. E 15, 699 (2006)
- [8] R.K. Gupta, M. Balasubramiam, R. Kumar, D. Singh, S. K. Arun and W. Greiner, J. Phys. G: Nucl. Part. Phys. 32, 345 (2006)
- [9] B.B. Singh, M.K. Sharma, R.K. Gupta, Phys. Rev. C 77, 054613 (2008)
- [10] R. Gupta, in proceedings of the 5th International Conference on Nuclear Research Mechanics, Varenna, 1988, edited by E. Gladioli, (Ricerca Scientifica ed Educazione Permanente, Milano, 1988), p.416.
- [11] S.S. Malik and R.K. Gupta, Phys. Rev. C 39, 1992 (1989)

- [12] R.K.Gupta, W.Scheid, and W.Greiner, J.Phys.G:Nucl. Part. Phys. 17,1731(1991).
- [13] S. Kumar and R.K.Gupta, Phys.Rev. C 49, 1922 (1994).
- [14] R.K.Gupta and W. Greiner Int. J. Mod. Phys. E 3, 335 (1994, Suppl.).
- [15] S. Kumar and R.K.Gupta, Phys. Rev. C 55, 218 (1997).
- [16] R.K. Gupta, in Heavy Elements and Related New Phenomena ,edited by W.Greiner and R.K Gupta (World Scientific Singapore) Vol.II ,p.730
- [17] S.K and R.K Gupta ,DAE nucl.Phys.(Sambalpur)52,365(2007)
- [18] B.B.Singh,S.K Arun, M.K.Sharma , S.Kanwar and Raj K.Gupta ,DAE Nucl.Phys.(Roorkee), Accepted(2008)
- [19] S. Yamaji, K.H. Ziegenhain, H.J. Fink, W. Greiner and W. Scheid, J. Phys.G: Nucl. Phys. 3, 1283 (1977).
- [20] R.K. Gupta, A. Sîandulescu and W. Greiner, Z. Naturforsch. 32a, 704 (1977).
- [21] R.K. Gupta, C. Pirvulescu, A. Sîandulescu and W. Greiner, Z. Phys. A 283,217 (1977); Sovt. J. Nucl. Phys. 28, 160 (1978).
- [22] R.K. Gupta, N.Singh, and M. Manhas, Phys. Rev. C 70, 034608 (2004)
- [23] R.K. Gupta ,M.balasubramaniam, R.Kumar, N.Singh, M.Manhas, and W. Greiner, J.Phys. G: Nucl.Part. Phys. C 31, 631(2005).
- [24] T. Matsuse, C. Beck, R. Nouicer, and D. Mahboub, Phys. Rev. C 55, 1380(1997).
- [25] S.J. Sanders, D.G. Kovar, B.B. Back, C. Beck, D.J. Henderson, R.V.F.Janssens, T.F. Wang, and B.D. Wilkins, Phys. Rev. C 40, 2091 (1989t).
- [26] S.J. Sanders, Phys. Rev. C 44, 2676 (1991).

- [27] J. Gomez del Campo, R.L. Auble, J.R. Beene, M.L. Halbert, H.J. Kim, A. D'Onofrio, and J.L. Charvet, Phys. Rev. C 43, 2689 (1991); Phys. Rev. Lett. 61, 290 (1988).
- [28] R.J. Charity, M.A. McMahan, G.J. Wozniak, R.J. McDonald, L. G. Moretto, D.G. Sarantites, L.G. Sobotka, G. Guarino, A. Pantaleo, L. Fiore, A. Gobbi and K.D. Hildenbrand, Nucl. Phys. A 483, 371 (1988).
- [29] C. Beck, R. Nouicer, D. Disdier, G. Duch[^]ene, G. de France, R.M. Freeman, F. Haas, A. Hachem, D. Mahboub, V. Rauch, M. Rousseau, S.J. Sanders, and A. Szanto de Toledo, Phys. Rev. C 63, 014607 (2001).
- [30] N.J. Davidson, S.S. Hsiao, J. Markram, H.G. Miller, and Y. Tzeng, Nucl. Phys. A 570, 61c (1994).
- [31] G. Audi and A.H. Wapstra, Nucl. Phys. A 595, 4 (1995).
- [32] G. Audi and A.H. Wapstra and C. Thiboult, Nucl. Phys. A 729, 337(2003)
- [33] P. M^oller, J. R. Nix, W. D. Myers, and W. J. Swiatecki, At. Data Nucl. Data Tables 59, 185 (1995).
- [34] W. Myers and W.J. Swiatecki, Nucl. Phys. 81, 1 (1966).
- [35] P. A. Seeger, Nucl. Phys. 25, 1 (1961)
- [36] H. Kroger and W. Scheid, J. Phys. G 6, L85(1980)
- [37] S.J. Sanders, D.G. Kovar, B.B. Back, C. Beck, B.K. Dichter, D. Henderson, R.V.F. Janssens, J.G. Keller, S. Kaufman, T.-F. Wang, B. Wilkins, and F. Videbaek, Phys. Rev. Lett. 59, 2856 (1987).

CHAPTER 3

RESULTS AND DISCUSSION

3.1 Introduction

The decay of heavy nuclear systems under the extreme condition of temperature, angular momentum etc has been of great interest in recent years. The availability of Radioactive nuclear beam has made it possible to investigate the nuclear structure and related properties in the new prospective and many new interesting concepts regarding the formation and decay of nuclear system has creped in. One of the important aspects in this category is the fusion hindrance. It is of upmost importance to investigate the fusion hindrance and its possible applications in reference to nuclear dynamics and related properties. Fusion hindrance in pre-actinide region is currently an active area of investigation in the field of heavy ion reactions. In the fusion hindrance, many collision trajectories lead to fission without reaching compound nucleus stage. These fission events are termed as noncompound nucleus (NCN) fission fragments. Suppression in the evaporation residue cross section [1-5], anomalous fission fragment angular distribution [6-11], and broadening in the fission fragment mass distribution [12, 13] are some of the possible signatures of fusion hindrance or NCN fission. Beside this some work has been done of asymmetric fission contributions coming from non compound nucleus states or related processes. The observed fusion hindrance in general is attributed to the lower entrance channel mass asymmetry (α) for these reaction systems compared to the Businaro-Gallone critical mass asymmetry (α_{BG}). However, a measurement of fission fragment angular distribution in the reactions $^{19}\text{F} + ^{197}\text{Au}$ and $^{24}\text{Mg} + ^{192}\text{Os}$ give contradictory result and do not show any significant contribution from noncompound nucleus fission. This observation was consistent with the pre-equilibrium fission model which predicted a small contribution from noncompound nucleus fission for these reaction systems. Therefore, the concept of fusion hindrance perhaps needs more investigation and understanding at least in the less fissile systems in the pre-actinide region.

In order to lode out for such aspects we hereby study the decay of $^{204}\text{Po}_{84}$ formed in $^{16}\text{O} + ^{188}\text{Os}$ reaction over a wide range of energies. The $Z_P Z_T$ value for the reaction $^{16}\text{O} + ^{188}\text{Os}$ is much lower than the onset of fusion hindrance. For the reaction $^{16}\text{O} + ^{188}\text{Os}$, measurements have been carried out at $E_{\text{lab}} = 84, 89, 94, 99$ MeV [14]

3.2 Results and discussion

In order to investigate the decay of $^{204}\text{Po}_{84}$ formed in $^{16}\text{O} + ^{188}\text{Os}$ reaction we have used Dynamical cluster decay model(DCM).The Dynamical cluster model is extremely successful in expanding various aspects of nuclear structure and dynamics related aspects related to ground state and excited state decays.

In the present work we have calculated ER and fission cross section at four reported energies for the decay of ^{204}Po formed in $^{16}\text{O} + ^{188}\text{Os}$ reaction. The DCM cross section comparison with Experimental data and other used parameters are given in Table 3.1. It is important to note that experimental data is fitted within one free parameter (ΔR), known as neck length parameter. As the experimental data was available individually for ER and fission so it has been fitted individually by taking appropriate ΔR values reported in table 3.1, the cross section are summed upto $l = l_{\text{max}}$ where reported l_{max} values are chosen at a point where $\sigma_{\text{ER}} \rightarrow 0$. As it is clear from table 3.1 the ΔR values are larger for ER as compared to that for fission. The results are discussed in fig. 3.5 the possible explanation is provided. Also, l_{max} for ΔR used to fit ER and slightly on lower side as compared to that for fission.

E_{LAB}	E_{CM}	l_{MAX} for ER(\hbar)	ΔR for ER	l_{MAX} for Fission (\hbar)	ΔR for Fission	σ_{ER} (DCM)	σ_{FISSION} (DCM)	σ_{CF} (DCM)	σ_{CF} (EXP)
84	77.411	123	1.8	132	0.98	222	53.4	275.4	285
89	82.019	123	1.86	132	1.1	331	171.6	502.6	499
94	86.627	108	1.908	108	1.39	321	384	705	691
99	91.235	124	1.85	129	1.5	276	570	846	863

Table 3.1 DCM calculated and Experimental cross sections for decay of ^{204}Po

Fig. 3.1 shows the fragmentation potential as a function of fragment mass at the extreme l values i.e. $l = 0$ and $l = l_{\text{max}}$. The sharp minima at ^{17}B shows the preference for

this cluster. However later in fig. 3.3 it has been shown that the penetrability of this cluster is extremely small so the dip at ^{17}B should not be taken so seriously. From fig. 3.1 it is clear that at $\ell = 0$ ER are more prominent whereas with increase in ℓ -value the fission fragments start competing with ER.

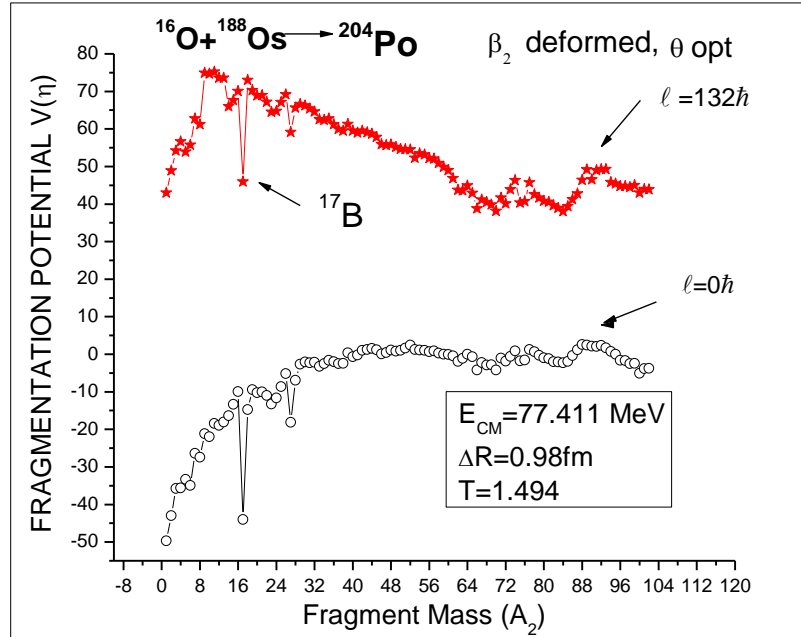


Fig. 3.1 Fragmentation potential as a function of fragment mass

Figure 3.2 shows the preformation graph for fission at $T=1.494\text{MeV}$ and $\Delta R = 0.98\text{fm}$. The preformation probability is the probability of formation of fragment and it reveals much needed structure information. The fragment mass distribution for the decay of ^{204}Po formed in $^{16}\text{O} + ^{188}\text{Os}$ channel is asymmetric in nature. Within the contributing fragments (asymmetric peak) there seems a double hump structure which gives rise to possibility of substructure among fission fragments.

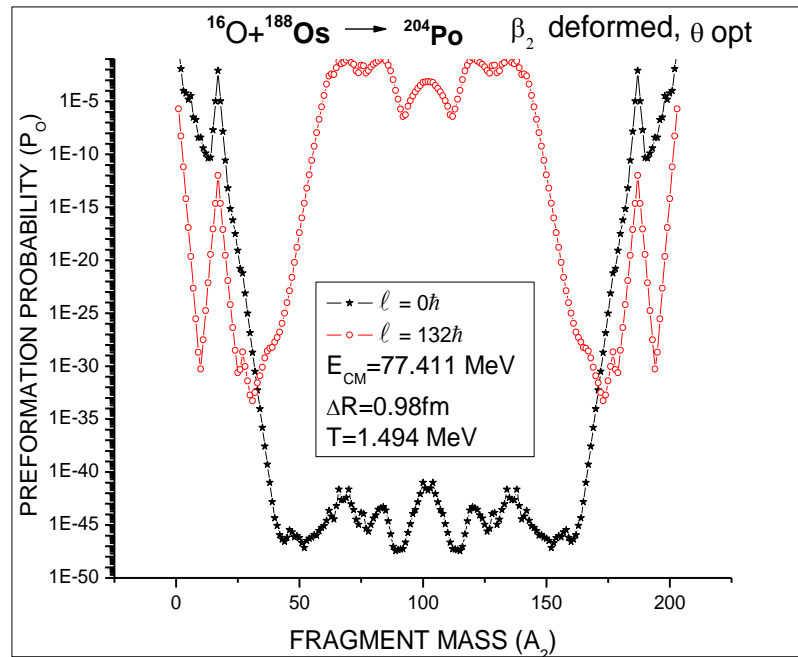


Fig. 3.2 Variation of Preformation probability as the function of mass fragments (A_2)

The Preformation graph is plotted at $\ell=0\hbar$ and $\ell_{\max}=132\hbar$. The fragments corresponding to $\ell_{\max}=132\hbar$ contributing to fission decay are 65-72 and 80-87.

Figure 3.3 shows the penetrability as the function of fragment mass number, calculated at $\ell=0\hbar$ and $\ell=132\hbar$ and $\Delta R=0.98$ fm and $T=1.494$ MeV. One may observe that penetrability of ^{17}B is negligibly small so preferential decay of ^{17}B (visible in fig. 3.1 and 3.2) gets ruled out completely due to extremely small value of Penetrability. The penetrability is calculated by using WKB approximation which depends on entry and exit points across the barrier as shown in fig. 3.4

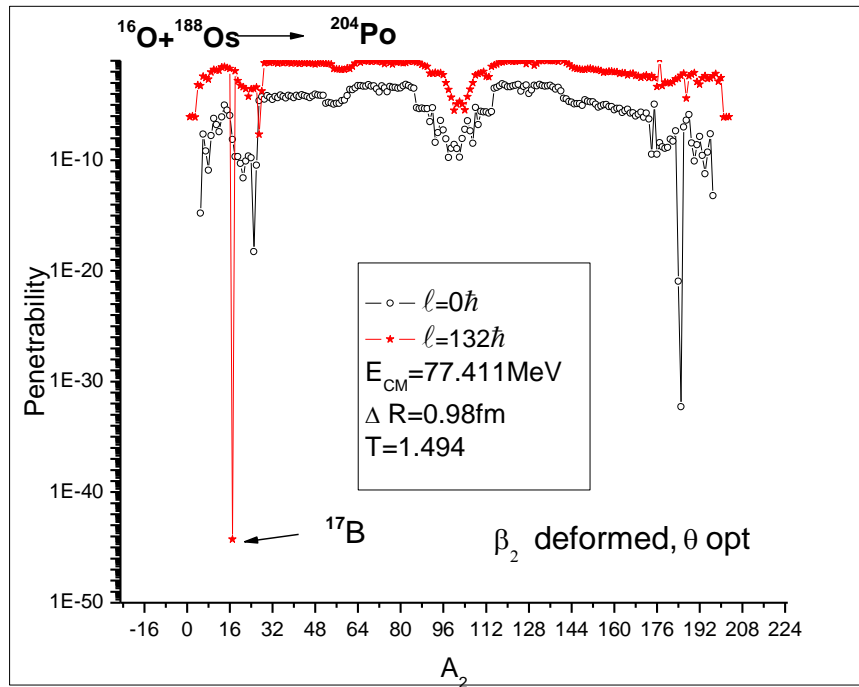


Fig. 3.3 Penetrability as the function of fragment mass number at $\ell=0\hbar$ and $\ell=132\hbar$

Fig. 3.4 shows the scattering potential behavior as a function of nuclear dimensions. In scattering graph, the first turning point of the penetrability path is at $R=R_a$ and the second turning point R_b is marked for the $\ell=0\hbar$ case of $R_a=R_t+\Delta R(T)$. The decay path for the ℓ -values begins at $R=R_a$.

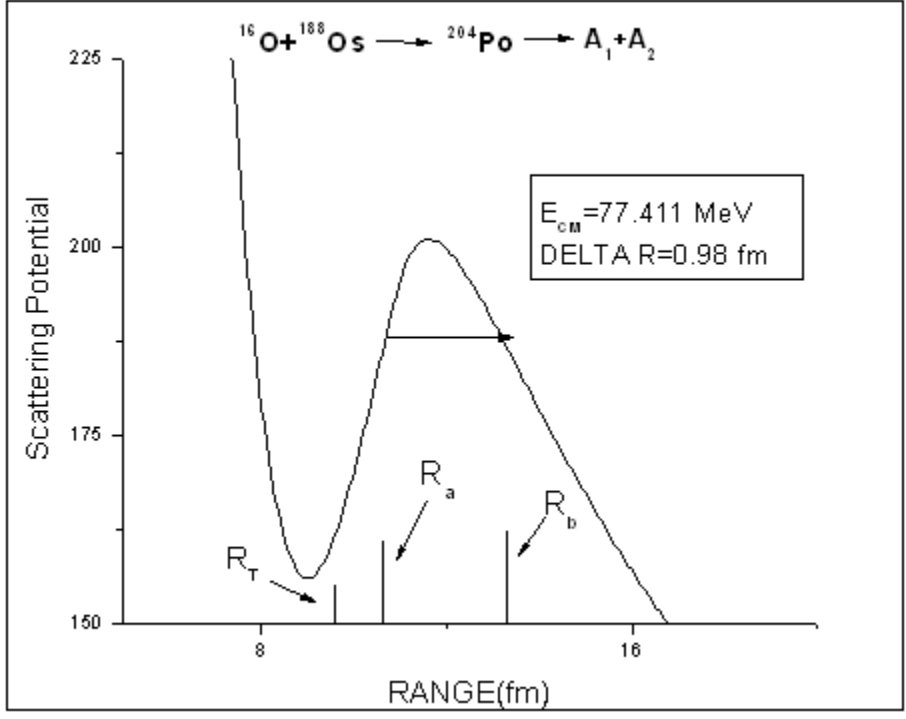


Fig. 3.4 Scattering Potential as a function of nuclear range

Fig. 3.5 shows the behavior of neck length parameter ΔR as a function of centre of mass energy E_{CM} for Evaporation Residue and Fission. The value of Delta R for Evaporation Residue is more than the Delta R of Fission which simply mean that ER occurs first followed by fission process. Therefore fig. 3.5 gives an exhibition of different time scales at which ER and fission processes take place.

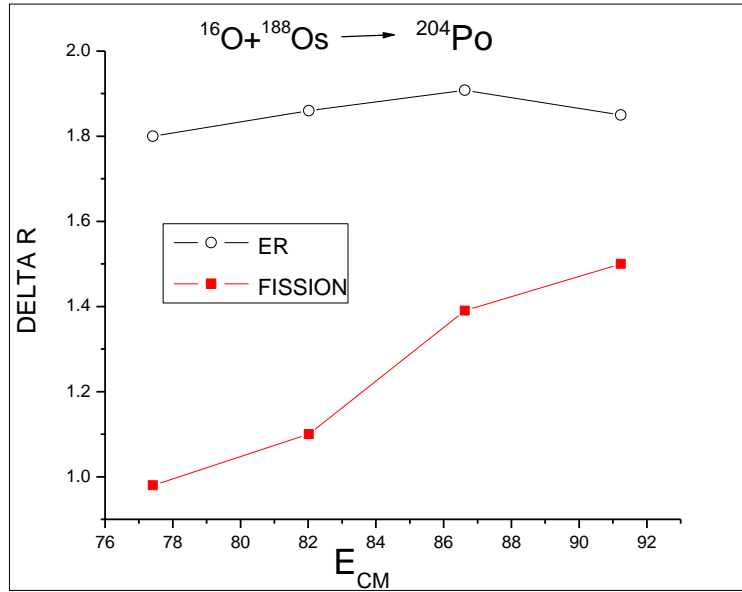


Fig. 3.5 Neck length parameter as a function of E_{CM}

Now, we compare the cross section calculated by DCM Model and experimental cross section. The total Fusion cross-sections are plotted at four different energies $E_{LAB} = 84, 89, 94$ and 99 MeV. Cross-section calculated by DCM model has very small deviation from Experimental cross-section and hence the results presented in this document are of extreme importance in reference to decay path of $^{204}\text{Po}_{84}$ nucleus. The individual calculated cross-sections corresponding to ER and Fission processes are also shown in figure 3.6. As we are able to fit the available experimental data with ER and fission contributions of possibility of non compound nucleus contribution in the decay of ^{204}Po formed in $^{16}\text{O} + ^{188}\text{Os}$ reaction is completely ruled out. Therefore the reaction under investigation doesn't lead to Fusion hindrance at the selected range of incident energies. It will be of further interest to take simultaneous ΔR values for ER and fission and then see the effect on Potential energy surfaces formed for $^{204}\text{Po}_{84}$ nucleus.

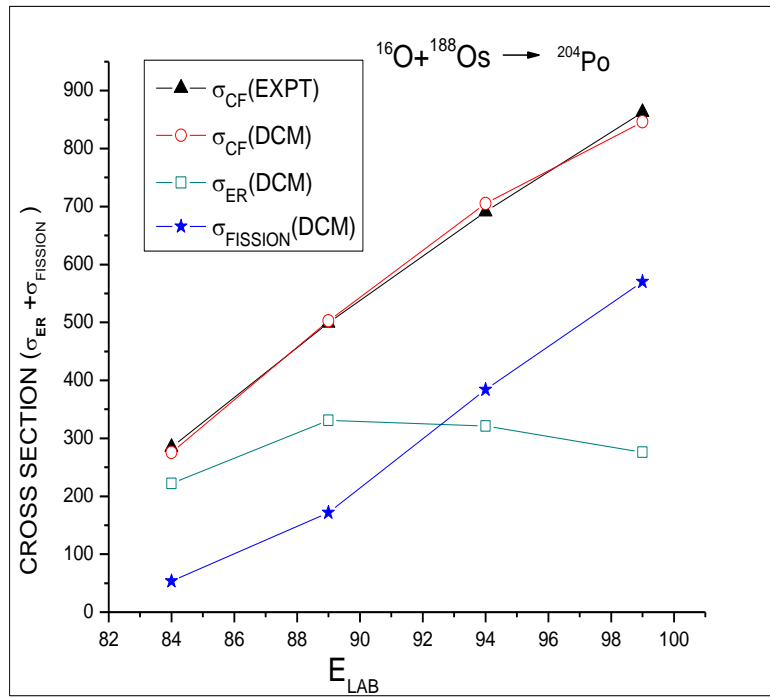


Fig. 3.6 Cross sections as a function of E_{CM}

3.3 References

- [1] K. Nishio *et al.*, Eur. Phys. J. A 29, 281 (2006).
- [2] S. Mitsuoka, H. Ikezoe, K. Nishio, K. Satou, and J. Lu, Phys. Rev. C 65, 054608 (2002).
- [3] K. Nishio, H. Ikezoe, Y. Nagame, M. Asai, K. Tsukada, S. Mitsuoka, K. Tsuruta, K. Satou, C. J. Lin, and T. Ohsawa, Phys. Rev. Lett. 93, 162701 (2004).
- [4] R. N. Sagaidak *et al.*, Phys. Rev. C 68, 014603 (2003).
- [5] M. Trotta *et al.*, Nucl. Phys. A787, 134 (2007).
- [6] J. P. Lestone, A. A. Sonzogni, M. P. Kelly, and R. Vandenbosch, Phys. Rev. C 56, R2907 (1997)
- [7] Bhivash R. Behera *et al.*, Phys. Rev. C 69, 064603 (2004).
- [8] G. N. Knyazheva *et al.*, Phys. Rev. C 75, 064602 (2007).
- [9] R. Tripathi, K. Sudarshan, S. Sodaye, S. K. Sharma, and A. V. R. Reddy, Phys. Rev. C 75, 024609 (2007).
- [10] B. B. Back, R. R. Betts, J. E. Gindler, B. D. Wilkins, S. Saini, M. B. Tsang, C. K. Gelbke, W. G. Lynch, M. A. McMahan, and P. A. Baisden, Phys. Rev. C 32, 195 (1985).
- [11] R. Tripathi, K. Sudarshan, S. Sodaye, A. V. R. Reddy, K. Mahata, and A.

Goswami, Phys. Rev. C 71, 044616 (2005).

[12] J. Toke *et al.*, Nucl. Phys. A440, 327 (1985).

[13] R. Rafiei *et al.*, Phys. Rev. C 77, 024606 (2008).

[14] R. Tripathi, K. Sudarshan, S. K. Sharma, K. Ramachandran, A. V. R. Reddy,
P. K. Pujari, and A. Goswami , PHYSICAL REVIEW C **79**, 064607 (2009).